How Does a Locally Constrained Quantum System Localize?

Chun Chen,[1] Fiona Burnell,[1] and Anushya Chandran[2,*]
[1]School of Physics and Astronomy, University of Minnesota, Minneapolis, Minnesota 55455, USA
[2]Department of Physics, Boston University, Boston, Massachusetts 02215, USA

(Received 14 September 2017; published 20 August 2018)

At low energy, the dynamics of excitations of many physical systems are locally constrained. Examples include frustrated antiferromagnets, fractional quantum Hall fluids, and Rydberg atoms in the blockaded regime. Can such locally constrained systems be fully many-body localized? In this Letter, we answer this question affirmatively and elucidate the structure of the accompanying quasilocal integrals of motion. By studying disordered spin chains subject to a projection constraint in the z direction, we show that full many-body localization (MBL) is stable at strong z-field disorder and identify a new mechanism of localization through resonance at strong transverse disorder. However, MBL is not guaranteed; the constraints can "frustrate" the tendency of the spins to align with the transverse fields and lead to full thermalization or criticality. We further provide evidence that the transition is discontinuous in local observables with large sample-to-sample variations. Our dynamical phase diagram is accessible in current Rydberg atomic experiments which realize programmable constrained Ising Hamiltonians.

DOI: 10.1103/PhysRevLett.121.085701

At low energy, the dynamics of many physical systems are restricted to Hilbert spaces with local constraints. For example, the canonical spin-ice compound $Dy_2Ti_2O_7$ has Ising-like magnetic moments that obey a local ice rule at low temperature [1,2]. Electronic systems such as fractional quantum Hall liquids and p-wave superconductors [3–10] are believed to host quasiparticles with non-Abelian statistics, which produce a topologically degenerate manifold of states within which the low energy dynamics are constrained. Finally, Rydberg excitations of cold atomic chains [11,12] are energetically forbidden to occupy adjacent sites in the blockaded regime.

Little is known about the dynamical phases of locally constrained systems in isolation [13–16]. Although their Hilbert space lacks a tensor product structure, there is a notion of locality because the influence of local measurements decays exponentially in space [13]. This suggests that constraints pose no impediment to local thermalization, as was numerically verified in pinned non-Abelian anyon chains [13] and in dimer models [14]. But what of the effects of spatial disorder? In unconstrained systems, quenched disorder can localize quantum particles and prevent the transport necessary for equilibration in isolation [17], a phenomenon known as many-body localization (MBL) [18–60]. In this Letter, we show that constraints pose no impediment to localization and present a model exhibiting new constraint-driven MBL and thermal phases (Fig. 1).

Local constraints have two opposing effects on potentially MBL systems. The constraints disallow certain intermediate states, blocking perturbative relaxation channels and yielding more robust localization. This is the case for the "diagonal MBL" phase in Fig. 1. However, when the constraints are transverse to the disorder, they may frustrate localization by forbidding extremal eigenstates of the disorder potential, effectively decreasing the energy detuning between adjacent spins. This effect partly underlies the robust energy transport in strongly disordered pinned non-Abelian anyon chains [16,61–67], and leads to the "constrained thermal" phase in Fig. 1. Surprisingly, such frustration does not preclude localization—in the

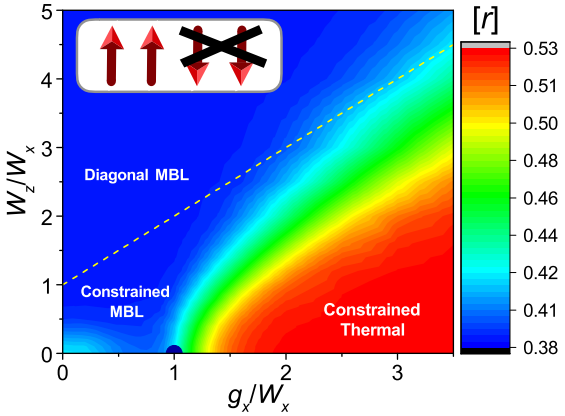

FIG. 1. Infinite temperature dynamical phase diagram of the constrained Ising model in Eq. (1) in which adjacent spins are forbidden to both point along $-z$ (inset). The mean level spacing ratio $[r]$ distinguishes the localized region with Poisson level statistics (blue, $[r] \approx 0.39$) from the thermalizing region with random matrix level statistics (red, $[r] \approx 0.53$). At large W_z/W_x, the localization transition approaches the dashed line (see text), while at small W_z/W_x, the transition line intersects the x axis at $g_x/W_x \approx 1$ (black dot).

"constrained MBL" phase, the spins in regions with weak potential are pinned such that nearby spins may resonate and become approximate eigenstates of the transverse disorder potential without violating the constraints. Thus, localization is favored by a mechanism reminiscent of "order-by-disorder" in frustrated spin systems [68].

Concretely, we study an open Ising chain of N spins whose Hilbert space $\tilde{\mathcal{H}}_N$ satisfies the constraint that neighboring spins cannot simultaneously point along $-z$ (see Fig. 1, inset). This Hilbert space describes quantum dimer ladders [69], pinned Fibonacci anyon chains [13,75], and Rydberg blockaded chains [76]. The dimension of $\tilde{\mathcal{H}}_N$ is given by F_{N+2}, where F_N is the Nth Fibonacci number. As $F_N \sim \phi^N$ with $\phi \equiv (\sqrt{5}+1)/2$ the golden mean for large N, the quantum dimension is irrational. The Hamiltonian of the system is

$$H = \sum_{i=1}^{N} (g_i \tilde{X}_i + h_i \tilde{Z}_i) \tag{1}$$

where g_i and h_i are independently drawn on each site from box distributions $g_x + [-W_x, W_x]$ and $[-W_z, W_z]$, respectively, and $\tilde{X}_i = P\sigma_i^x P$, $\tilde{Z}_i = P\sigma_i^z P$ are the projected Pauli operators $\sigma_i^{x,z}$ on site i. The projection operator P annihilates any z configuration with the $\downarrow\downarrow$ motif,

$$P = \prod_i \frac{(3 + \sigma_i^z + \sigma_{i+1}^z - \sigma_i^z \sigma_{i+1}^z)}{4}, \tag{2}$$

so that $\tilde{X}_i$ can flip spin i only if $\tilde{Z}_{i-1} = \tilde{Z}_{i+1} = 1$. Without constraints, each spin independently precesses around its local field and there is neither transport of energy, nor local equilibration. The constraints force neighboring spins to interact as $[\tilde{X}_i, \tilde{X}_{i+1}] \neq 0$, producing the rich dynamical phase diagram in Fig. 1.

The diagonal MBL phase.—The restriction to $\tilde{\mathcal{H}}_N$ is trivial when H is diagonal in the z basis ($g_i \equiv 0$). This diagonal limit is localized; every eigenstate $|E\rangle$ is uniquely labeled by the string of its ± 1 eigenvalues under the operators, $\tilde{Z}_i$ for $i = 1, \ldots, N$. The strings satisfy the constraint

$$|E\rangle = |\{\tilde{Z}_i\}\rangle, \qquad \tilde{Z}_i \quad \text{and} \quad \tilde{Z}_{i+1} \neq -1. \tag{3}$$

The local conserved operators $\tilde{Z}_i$ define *l-bits*, which unlike their unconstrained counterparts, satisfy a restricted algebra wherein $\tilde{Z}_i \tilde{Z}_{i+1} = \tilde{Z}_i + \tilde{Z}_{i+1} - \mathbb{1}$. This implies that the subset of all possible tensor product operators which do not contain both $\tilde{Z}_i$ and $\tilde{Z}_{i+1}$ for any i form a basis for the F_{N+2} conserved operators [69].

Imbrie [50,77] rigorously showed that the closely related unconstrained model

$$H_{\mathrm{IM}} = \sum_{i=1}^{N} g_i \sigma_i^x + h_i \sigma_i^z + J_i \sigma_i^z \sigma_{i+1}^z \tag{4}$$

can be diagonalized using a sequence of quasilocal unitary operators U. Since terms containing r spins appear in the generator of U with an amplitude that is (with high probability) exponentially small in r, the l-bits at $g_i = 0$ extend to quasilocal l-bits at small g_i: $\tau_i^z \equiv U\sigma_i^z U^\dagger$. These l-bits underlie the integrability, the dephasing dynamics, and the low eigenstate entanglement of the fully MBL phase [26,30,48–54].

The above arguments can be adapted to argue for full MBL in our model when $g_x, W_x \ll W_z$ (upper-left corner of Fig. 1). Specifically, as (i) the constraints do not affect the level statistics of the spectrum of the diagonal limit at $g_i = 0$, and (ii) certain terms only appear in the rotated Hamiltonian at higher order in perturbation theory as compared to the unconstrained case, we can perturbatively construct a quasilocal unitary U which diagonalizes Eq. (1) with high probability and defines l-bits: $\tilde{\tau}_i^z = U\tilde{Z}_i U^\dagger$ with the same properties as Eq. (3) in the diagonal limit. U also defines the quasilocal operator $\tilde{\tau}_i^x$ that flips the z eigenvalue of the l-bit i: $\tilde{\tau}_i^x = U\tilde{X}_i U^\dagger$. As in the diagonal limit, $[\tilde{\tau}_i^x, \tilde{\tau}_{i\pm1}^x] \neq 0$.

We support these claims with exact diagonalization performed on $N_s \geq 1000$ samples at $N = 14$–18 and $N_s = 500$ samples at $N = 20$. Within each sample, we consider the central third of the sites and the central third of the eigenspectrum. At large W_z, we expect that the l-bit $\tilde{\tau}_i^z$ is a weakly dressed version of $\tilde{Z}_i$ with a finite fraction of its operator weight on $\tilde{Z}_i$. As $\langle E|\tilde{\tau}_i^z|E\rangle = \pm 1$, we expect a bimodal distribution for $\langle E|\tilde{Z}_i|E\rangle$ with weight primarily at ± 1 as $N \to \infty$. This is confirmed by Fig. 2(a). The (small) weight between -0.5 and 0.5 comes from eigenstates in which spins $i-1$ and $i+1$ point primarily along $+z$, so that spin i points along or against its local field direction. As the local field is in the x-z plane, the z projection of spin i is reduced [69].

The constrained thermal phase.—When the maximum x field $g_x + W_x$ is comparable to the typical z field $\sim W_z$, the perturbative construction of the quasilocal unitary breaks down and a thermal phase emerges. This suggests that the phase boundary lies at $W_z/W_x \sim g_x/W_x + 1$ for large W_z/W_x (dashed line in Fig. 1). The constrained thermal phase persists to small W_z/W_x for $g_x/W_x \gg 1$, in agreement with the intuition that weakly disordered, strongly interacting models thermalize. Indeed Fig. 2(d) confirms that the model satisfies the eigenstate thermalization hypothesis (ETH) [78–82] expected of thermalizing phases, in which individual eigenstates reproduce the expectation values of the thermal ensemble [69]. Specifically, panel (d) shows that $P(\langle E|\tilde{Z}_i|E\rangle)$ concentrates around the infinite temperature value of $1/\sqrt{5}$ with increasing N, in contrast to the distribution in the MBL phase in panel (a).

The constrained MBL phase.—Strikingly, numerical signatures of localization persist in the lower left corner of Fig. 1 (g_x, $W_z \ll W_x$), when the x field dominates the z field on most sites. As adjacent spins *cannot*

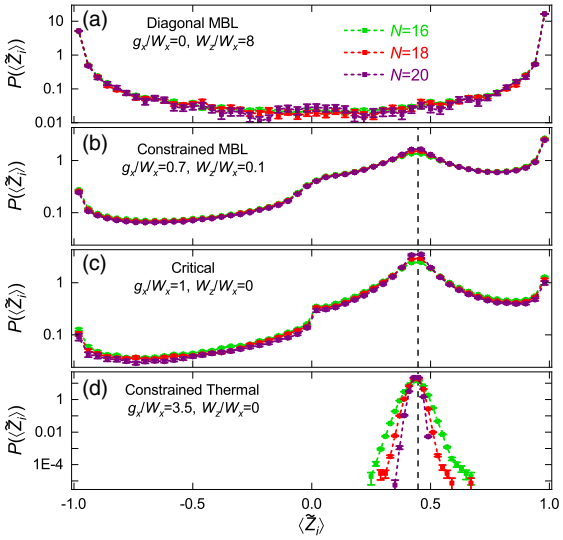

FIG. 2. Probability distribution of $\langle E|\tilde{Z}_i|E\rangle$. In the diagonal MBL phase [panel (a)], the distribution is bimodal with maxima near ± 1. In the constrained thermal phase [panel (d)], the distribution concentrates around the infinite temperature average of $1/\sqrt{5}$ (dashed line). In the constrained MBL phase [panel (b)] and at the transition [panel (c)], the distribution shows features of both MBL and thermal phases.

simultaneously align or antialign in the x direction ($[\tilde{X}_i, \tilde{X}_{i+1}] \neq 0$), the mechanism underlying localization must be qualitatively different than in the diagonal MBL phase. To expose this mechanism, consider a 3-site chain with $g_1 \neq g_3 > 0$, but $g_2 = 0$. There are five eigenstates: four of them $|\tilde{X}_1 = \pm 1, \tilde{Z}_2 = 1, \tilde{X}_3 = \pm 1\rangle$ have energies $\pm g_1 \pm g_3$, while the fifth $|\tilde{Z}_1 = -1, \tilde{Z}_2 = 1, \tilde{Z}_3 = -1\rangle$ has zero energy. In other words, the x fields on sites 1 and 3 create an effective z field of order $|g_3 - g_1|$ on site 2. If $|g_2| \ll |g_3 - g_1|$, $\tilde{Z}_2$ will be approximately conserved.

In the model in Eq. (1) with strong and weak x-field segments of varying length, a similar mechanism can generate effective z fields on sites with weak x fields. The Hamiltonian on a finite strong segment satisfies the ETH; the effective z field on an adjacent weak x-field site i is therefore set by the level spacing of the strong segment. When this effective z field exceeds g_i (i.e., when the segments are not too long), we expect that $\tilde{Z}_i \approx \pm 1$ in all eigenstates. At $W_z > 0$, the bare z fields stabilize this constrained MBL phase in two ways: (i) they add to the z field on weak sites, and (ii) they increase the strength of the effective z field generated by strong segments by decreasing the length of the typical strong segments. Once the typical z field exceeds the x field on each site, the system smoothly crosses over into the diagonal MBL phase. Figure 2(b) confirms this picture: the distribution $\langle E|\tilde{Z}_i|E\rangle$ shows significant weight at ± 1, coming from weak x-field sites that are pinned in the z direction. The strong segments account for the weight near the thermal value of $1/\sqrt{5}$. The lack of concentration of measure around the thermal value with increasing N indicates that the length of the strong segments is finite (see the Supplemental Material for further details [69]).

At $W_z = 0$, atypically long strong segments may destabilize the localized phase through avalanche effects [83]. Numerically, the proximity to the thermal transition also complicates the interpretation of the data at $W_z = 0$, $g_x/W_x < 1$, as we discuss below. We now show that without such rare segments, our argument for localization can be made rigorous. To this end, consider the strong-weak-strong (SWS) model obtained from Eq. (1) by taking $h_i = 0$ and repeating the 3-site x-field motif discussed above:

$$g_i \in \begin{cases} [-\delta_w, \delta_w], & \text{if } i = 0 \bmod 3 \\ [1-\delta_s, 1+\delta_s], & \text{otherwise.} \end{cases} \tag{5}$$

For $\delta_w = 0$, the local operators $\hat{O}_{3i} = g_{3i+1}X_{3i+1} + g_{3i+2}X_{3i+2}$ and $\tilde{Z}_{3i}$ commute with one another and with H. The eigenvalues $\epsilon_{3i} = 0, \pm g_{3i+1}, \pm g_{3i+2}, \pm\sqrt{g_{3i+1}^2 + g_{3i+2}^2}$ of the $\hat{O}_{3i}$ uniquely label the eigenstates, and the energies are given by $\sum_{3i}\epsilon_{3i}$. Thus, this model is trivially localized with conserved operators given by $\{\hat{O}_{3i}\}$.

In the Supplemental Material [69], we again adapt the methods of Refs. [50,77] to argue that full MBL persists for $\delta_w \ll \delta_s$ in the SWS model. Specifically, as the energy spectrum obeys limited level attraction at $\delta_w = 0$, and resonances can occur only if two nearby strong fields differ by an amount $\sim\delta_w$, there exists a quasilocal unitary that diagonalizes H and defines a set of l-bits at small δ_w. This demonstrates that fields that commute with the constraint are not, in general, necessary for localization.

The line $W_z = 0$.—For $W_z = 0$, the minimum x field given by $g_x - W_x$ controls the phase diagram. When $g_x > W_x$, there are no weak x fields and we expect thermalization, while for $g_x < W_x$, we expect a constrained MBL phase up to rare region effects. In Fig. 3, we use two measures to test this: (a) the mean level spacing ratio $[r]$ [22,84], and (b) the mean half-chain entanglement entropy $[S]$. $r(n)$ is defined as $\min(\delta(n), \delta(n+1))/\max(\delta(n), \delta(n+1))$ with $\delta(n) = E_n - E_{n-1}$ when the energies E_i are enumerated in increasing order, while S is defined as $-\mathrm{Tr}\rho_L \log_2 \rho_L$, where ρ_L is the reduced density matrix of the left half of the chain in eigenstate $|E\rangle$. The mean is taken with respect to sites, states, and samples and the normalization S_P is the finite-size corrected entropy [85] of an infinite temperature state [86]. The finite-size flow of $[r]$ and $[S]/S_P$ towards their respective thermal values of r_{GOE} and 1, where r_{GOE} is the value of $[r]$ in a Gaussian orthogonal ensemble, confirms the thermal phase for $g_x > W_x$.

In the constrained MBL phase, we expect $[r] \to r_{\mathrm{Poi}}$ and $[S]/S_P \to 0$ with increasing N. While $[r]$ exhibits some finite-size flow towards r_{Poi} for $g_x < W_x$ in Fig. 3, there is little flow in $[S]/S_P$. This is likely due to the proximity to the (same) transition at $g_x = 0$ and $g_x = W_x$. Since

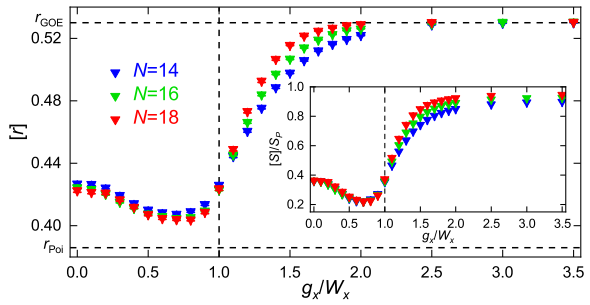

FIG. 3. $[r]$ (main plot) and $[S]/S_P$ (inset) for $W_z = 0$. Both quantities approach their respective thermal values of r_{GOE} and 1 with increasing N for $g_x/W_x > 1$, suggesting that the transition is at $g_x/W_x = 1$ in the thermodynamic limit.

performing local rotations about the z axis on sites with $g_i < 0$ yields an equivalent model with strictly positive x fields, $g_x = 0$ and $g_x = W_x$ represent the same dynamical transition: there is a sample at $g_x = W_x$ for every sample at $g_x = 0$ with the same eigenstate properties. Whether rare region effects are also important will be addressed in future work [87].

At the purported transition $g_x/W_x = 1$, the distribution of $\langle E|\tilde{Z}_i|E\rangle$ in Fig. 2(c) exhibits sharp features at four values: ± 1, 0, and at the infinite temperature value of $1/\sqrt{5}$. That is, spins either point along $\pm z$, $\pm x$, or are locally thermal in eigenstates. The thermal peak height increases with increasing N, while the other features persist, suggesting that (i) the transition point is heterogenous with respect to local observables, and (ii) eigenstate expectation values of local observables jump across $g_x/W_x = 1$.

In order to determine the origin of the striking heterogeneity, we use different evaluations of the normalized standard deviation $\Delta S/S_P$ following Ref. [88]. Figure 4 shows three possibilities: (i) intersample $\Delta_s[S]_{E,c}$, (ii) intrasample across eigenstates $[\Delta_E[S]_c]_s$, and (iii) intrasample across the position of the cuts $[\Delta_c S]_{E,s}$, where s, E, c, respectively, refer to sample, eigenstates, and cuts. In the thermal phase for $g_x/W_x > 1$, all three quantities go to zero with increasing N, showing that S for any position of the cut in any eigenstate in any sample is representative of the

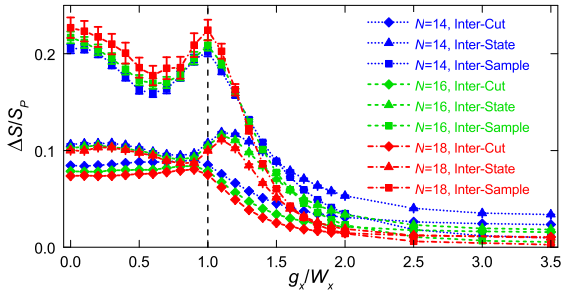

FIG. 4. Normalized standard deviation of the half chain entanglement entropy $\Delta S/S_P$ at $W_z = 0$ parsed by samples, states, and cuts, showing that the largest contribution comes from the intersample variance near $g_x/W_x = 1$.

phase. At $g_x/W_x = 1$, on the other hand, the intersample deviation dominates and even slightly increases with N, while the other two variations decrease with N. This strongly suggests that the transition is like an equilibrium first-order transition [89,90] in which all of the variation in S comes from intersample variation in the x fields. This scenario has been suggested by several works [88,91–93], and our model provides the first clear microscopic observation. We note that the increase in $\Delta_s[S]_{E,c}/S_P$ with N cannot indefinitely continue as the variable is bounded.

Discussion.—We have studied the fate of MBL in a constrained disordered system, and found that constraints can either assist or frustrate localization, depending on whether or not they commute with the random fields. We have also shown by explicit construction that random fields transverse to the constraint lead to localization through a new resonance mechanism. Finally, we have provided strong evidence that the transition out of the thermal phase is "first-order," in the sense that the primary variation of the half-chain entanglement entropy comes from intersample variation and that local observables vary discontinuously across the transition.

There are a number of interesting directions for further study. Recently, Ref. [66] argued that MBL is impossible in pinned non-Abelian anyon chains, partly due to the lack of a tensor product Hilbert space. Since we have shown that constraints alone do not prevent localization, this delocalization must be a consequence of the $SU(2)_k$ symmetry respected by the anyon Hamiltonians. Constrained models may also provide simpler realizations of the nonergodic delocalized phase posited in the non-Abelian systems [65].

The large intersample variation in S at the numerically accessible system sizes suggests that the numerically extracted finite-size scaling exponents will obey the Harris criterion [38,94], in sharp contrast to the numerical exponents reported for unconstrained models [35,37,95]. More broadly, as the nonthermal behavior for small W_z results from weak x fields, the constrained Ising model provides a unique setting to isolate the effects of rare regions. Since Eq. (1) describes Rydberg-blockaded chains, quenches and other dynamical experiments [12] in the presence of disorder should access these rare region effects in energy transport and in entanglement growth.

We are grateful to C. R. Laumann, S. L. Sondhi, and D. Huse for stimulating discussions and for a careful reading of the manuscript, and to P. Crowley and V. Khemani for helpful conversations. F. J. B. acknowledges the financial support of NSF DMR-1352271, and of the Alfred P. Sloan Foundation FG-2015-65927.

*anushyac@bu.edu

[1] C. Castelnovo, R. Moessner, and S. Sondhi, Annu. Rev. Condens. Matter Phys. **3**, 35 (2012).

[2] M. J. P. Gingras and P. A. McClarty, Rep. Prog. Phys. **77**, 056501 (2014).
[3] G. Moore and N. Read, Nucl. Phys. **B360**, 362 (1991).
[4] D. A. Ivanov, Phys. Rev. Lett. **86**, 268 (2001).
[5] A. Y. Kitaev, Phys. Usp. **44**, 131 (2001).
[6] Y. Oreg, G. Refael, and F. von Oppen, Phys. Rev. Lett. **105**, 177002 (2010).
[7] R. M. Lutchyn, J. D. Sau, and S. Das Sarma, Phys. Rev. Lett. **105**, 077001 (2010).
[8] M. Barkeshli and X.-L. Qi, Phys. Rev. X **4**, 041035 (2014).
[9] M. Cheng, Phys. Rev. B **86**, 195126 (2012).
[10] N. H. Lindner, E. Berg, G. Refael, and A. Stern, Phys. Rev. X **2**, 041002 (2012).
[11] A. M. Kaufman, B. J. Lester, C. M. Reynolds, M. L. Wall, M. Foss-Feig, K. R. A. Hazzard, A. M. Rey, and C. A. Regal, Science **345**, 306 (2014).
[12] H. Bernien *et al.*, Nature (London) **551**, 579 (2017).
[13] A. Chandran, M. D. Schulz, and F. J. Burnell, Phys. Rev. B **94**, 235122 (2016).
[14] Z. Lan and S. Powell, Phys. Rev. B **96**, 115140 (2017).
[15] M. Brenes, M. Dalmonte, M. Heyl, and A. Scardicchio, Phys. Rev. Lett. **120**, 030601 (2018).
[16] A. Prakash, S. Ganeshan, L. Fidkowski, and T.-C. Wei, Phys. Rev. B **96**, 165136 (2017).
[17] P. W. Anderson, Phys. Rev. **109**, 1492 (1958).
[18] L. Fleishman and P. W. Anderson, Phys. Rev. B **21**, 2366 (1980).
[19] B. L. Altshuler, Y. Gefen, A. Kamenev, and L. S. Levitov, Phys. Rev. Lett. **78**, 2803 (1997).
[20] D. Basko, I. Aleiner, and B. Altshuler, Ann. Phys. (Amsterdam) **321**, 1126 (2006).
[21] I. V. Gornyi, A. D. Mirlin, and D. G. Polyakov, Phys. Rev. Lett. **95**, 206603 (2005).
[22] V. Oganesyan and D. A. Huse, Phys. Rev. B **75**, 155111 (2007).
[23] C. Monthus and T. Garel, Phys. Rev. B **81**, 134202 (2010).
[24] R. Vosk and E. Altman, Phys. Rev. Lett. **110**, 067204 (2013).
[25] D. Pekker, G. Refael, E. Altman, E. Demler, and V. Oganesyan, Phys. Rev. X **4**, 011052 (2014).
[26] A. Pal and D. A. Huse, Phys. Rev. B **82**, 174411 (2010).
[27] M. Žnidarič, T. Prosen, and P. Prelovšek, Phys. Rev. B **77**, 064426 (2008).
[28] J. H. Bardarson, F. Pollmann, and J. E. Moore, Phys. Rev. Lett. **109**, 017202 (2012).
[29] M. Serbyn, Z. Papić, and D. A. Abanin, Phys. Rev. Lett. **110**, 260601 (2013).
[30] B. Bauer and C. Nayak, J. Stat. Mech. (2013) P09005.
[31] B. Swingle, arXiv:1307.0507.
[32] R. Nandkishore, S. Gopalakrishnan, and D. A. Huse, Phys. Rev. B **90**, 064203 (2014).
[33] M. Serbyn, Z. Papić, and D. A. Abanin, Phys. Rev. B **90**, 174302 (2014).
[34] S. Iyer, V. Oganesyan, G. Refael, and D. A. Huse, Phys. Rev. B **87**, 134202 (2013).
[35] J. A. Kjäll, J. H. Bardarson, and F. Pollmann, Phys. Rev. Lett. **113**, 107204 (2014).
[36] C. R. Laumann, A. Pal, and A. Scardicchio, Phys. Rev. Lett. **113**, 200405 (2014).
[37] D. J. Luitz, N. Laflorencie, and F. Alet, Phys. Rev. B **91**, 081103 (2015).
[38] A. Chandran, C. R. Laumann, and V. Oganesyan, arXiv: 1509.04285.
[39] B. Tang, D. Iyer, and M. Rigol, Phys. Rev. B **91**, 161109 (2015).
[40] V. P. Michal, B. L. Altshuler, and G. V. Shlyapnikov, Phys. Rev. Lett. **113**, 045304 (2014).
[41] K. Agarwal, S. Gopalakrishnan, M. Knap, M. Müller, and E. Demler, Phys. Rev. Lett. **114**, 160401 (2015).
[42] R. Vasseur, S. A. Parameswaran, and J. E. Moore, Phys. Rev. B **91**, 140202 (2015).
[43] R. Singh, J. H. Bardarson, and F. Pollmann, New J. Phys. **18**, 023046 (2016).
[44] Y.-Z. You, X.-L. Qi, and C. Xu, Phys. Rev. B **93**, 104205 (2016).
[45] A. C. Potter, R. Vasseur, and S. A. Parameswaran, Phys. Rev. X **5**, 031033 (2015).
[46] R. Nandkishore and D. A. Huse, Annu. Rev. Condens. Matter Phys. **6**, 15 (2015).
[47] E. Altman and R. Vosk, Annu. Rev. Condens. Matter Phys. **6**, 383 (2015).
[48] D. A. Huse, R. Nandkishore, and V. Oganesyan, Phys. Rev. B **90**, 174202 (2014).
[49] M. Serbyn, Z. Papić, and D. A. Abanin, Phys. Rev. Lett. **111**, 127201 (2013).
[50] J. Z. Imbrie, J. Stat. Phys. **163**, 998 (2016).
[51] V. Ros, M. Müller, and A. Scardicchio, Nucl. Phys. **B891**, 420 (2015).
[52] A. Chandran, I. H. Kim, G. Vidal, and D. A. Abanin, Phys. Rev. B **91**, 085425 (2015).
[53] C. Monthus, J. Stat. Mech. (2016) 033101.
[54] L. Rademaker and M. Ortuño, Phys. Rev. Lett. **116**, 010404 (2016).
[55] A. Nanduri, H. Kim, and D. A. Huse, Phys. Rev. B **90**, 064201 (2014).
[56] L. Zhang, H. Kim, and D. A. Huse, Phys. Rev. E **91**, 062128 (2015).
[57] M. Serbyn, M. Knap, S. Gopalakrishnan, Z. Papić, N. Y. Yao, C. R. Laumann, D. A. Abanin, M. D. Lukin, and E. A. Demler, Phys. Rev. Lett. **113**, 147204 (2014).
[58] N. Y. Yao, C. R. Laumann, and A. Vishwanath, arXiv:1508 .06995.
[59] A. Chandran, V. Khemani, C. R. Laumann, and S. L. Sondhi, Phys. Rev. B **89**, 144201 (2014).
[60] Y. Bahri, R. Vosk, E. Altman, and A. Vishwanath, Nat. Commun. **6**, 7341 (2015).
[61] L. Fidkowski, H.-H. Lin, P. Titum, and G. Refael, Phys. Rev. B **79**, 155120 (2009).
[62] Y. E. Kraus and A. Stern, New J. Phys. **13**, 105006 (2011).
[63] C. R. Laumann, D. A. Huse, A. W. W. Ludwig, G. Refael, S. Trebst, and M. Troyer, Phys. Rev. B **85**, 224201 (2012).
[64] C. R. Laumann, A. W. W. Ludwig, D. A. Huse, and S. Trebst, Phys. Rev. B **85**, 161301 (2012).
[65] R. Vasseur, A. C. Potter, and S. A. Parameswaran, Phys. Rev. Lett. **114**, 217201 (2015).
[66] A. C. Potter and R. Vasseur, Phys. Rev. B **94**, 224206 (2016).
[67] B. Kang, A. C. Potter, and R. Vasseur, Phys. Rev. B **95**, 024205 (2017).
[68] J. Villain, R. Bidaux, J.-P. Carton, and R. Conte, J. Phys. (Les Ulis, Fr.) **41**, 1263 (1980).

[69] See Supplemental Material at http://link.aps.org/supplemental/10.1103/PhysRevLett.121.085701 for derivations of several results mentioned in the main text, as well as additional numerical data, which includes Refs. [70–74].
[70] B. I. Shklovskii, B. Shapiro, B. R. Sears, P. Lambrianides, and H. B. Shore, Phys. Rev. B **47**, 11487 (1993).
[71] R. Moessner and S. L. Sondhi, Phys. Rev. B **63**, 224401 (2001).
[72] C. R. Laumann, R. Moessner, A. Scardicchio, and S. L. Sondhi, Phys. Rev. Lett. **109**, 030502 (2012).
[73] D. S. Rokhsar and S. A. Kivelson, Phys. Rev. Lett. **61**, 2376 (1988).
[74] R. Moessner and K. S. Raman, arXiv:0809.3051.
[75] S. Trebst, M. Troyer, Z. Wang, and A. W. W. Ludwig, Prog. Theor. Phys. Suppl. **176**, 384 (2008).
[76] D. Comparat and P. Pillet, J. Opt. Soc. Am. B **27**, A208 (2010).
[77] J. Z. Imbrie, Phys. Rev. Lett. **117**, 027201 (2016).
[78] R. V. Jensen and R. Shankar, Phys. Rev. Lett. **54**, 1879 (1985).
[79] J. M. Deutsch, Phys. Rev. A **43**, 2046 (1991).
[80] M. Srednicki, Phys. Rev. E **50**, 888 (1994).
[81] M. Rigol, V. Dunjko, and M. Olshanii, Nature (London) **452**, 854 (2008).
[82] L. D'Alessio, Y. Kafri, A. Polkovnikov, and M. Rigol, Adv. Phys. **65**, 239 (2016).
[83] W. De Roeck and F. Huveneers, Phys. Rev. B **95**, 155129 (2017).
[84] Y. Y. Atas, E. Bogomolny, O. Giraud, and G. Roux, Phys. Rev. Lett. **110**, 084101 (2013).
[85] D. N. Page, Phys. Rev. Lett. **71**, 1291 (1993).
[86] For our model $S_P \equiv \log_2(\dim(\rho_A)) - 1/(2\ln 2) \equiv \log(F_{N/2+2}) - 1/(2\ln 2)$. Numerically we find that the entropy of a random state in $\tilde{\mathcal{H}}$ is $S_T \approx S_P - 0.06$.
[87] C. Chen, A. Chandran, and F. J. Burnell (to be published).
[88] V. Khemani, S. P. Lim, D. N. Sheng, and D. A. Huse, Phys. Rev. X **7**, 021013 (2017).
[89] M. E. Fisher and A. N. Berker, Phys. Rev. B **26**, 2507 (1982).
[90] F. Pázmándi, R. T. Scalettar, and G. T. Zimányi, Phys. Rev. Lett. **79**, 5130 (1997).
[91] X. Yu, D. J. Luitz, and B. K. Clark, Phys. Rev. B **94**, 184202 (2016).
[92] P. T. Dumitrescu, R. Vasseur, and A. C. Potter, Phys. Rev. Lett. **119**, 110604 (2017).
[93] P. Ponte, C. R. Laumann, D. A. Huse, and A. Chandran, Phil. Trans. R. Soc. A **375**, 20160428 (2017).
[94] J. T. Chayes, L. Chayes, D. S. Fisher, and T. Spencer, Phys. Rev. Lett. **57**, 2999 (1986).
[95] V. Khemani, D. N. Sheng, and D. A. Huse, Phys. Rev. Lett. **119**, 075702 (2017).